Ultrasonic vibration assisted Electro-jet machining for macro to micro drilling applications of thin metal sheets/foils

A thesis submitted in partial fulfilment
of the requirements for the award of the degree of

Bachelor of Technology

in

Mechanical Engineering

and

Master of Technology

in

Manufacturing Engineering

Submitted by

D Krishna Vamsi
17ME02028

Under the Supervision of
Dr. Suvradip Mullick
Assistant Professor, SMS

School of Mechanical Sciences
Indian Institute of Technology, Bhubaneswar
Argul, Jatni, Bhubaneswar – 752050

2021-2022

June 2022.

यांत्रिकी विज्ञान विद्यापीठ/School of Mechanical Sciences
भारतीय प्रौद्योगिकी संस्थान भुवनेश्वर/Indian Institute of Technology Bhubaneswar
जटनी - 752050/Jatni–752050,**खोर्धा/** Khordha,**ओड़िशा**, **भारत/** Odisha, India

APPROVAL OF THE VIVA-VOCE BOARD

Date:20/06/2022

Certified that the thesis entitled "**Ultrasonic vibration assisted Electro-jet machining for macro-micro drilling applications of metal sheets/foils**" submitted by "**D Krishna Vamsi**", a Dual Degree student of B.Tech. in Mechanical Engineering and MTech. in Manufacturing Engineering, to the School of Mechanical Sciences, Indian Institute of Technology, Bhubaneswar for the award of Master of Technology degree has been accepted by the internal and external examiner/examiners. The student has successfully defended his thesis in the viva-voice examination.

Dr. Suvradip Mullick
(Supervisor)

Dr. Gaurav Bartarya
(Supervisor)

Dr. M M Mahapatra
(Internal Examiner)

Dr. Chetan
(Internal Examiner)

(External Examiner)

Dr. M M Mahapatra
(Head of the School)

यांत्रिकी विज्ञान विद्यापीठ/School of Mechanical Sciences
भारतीय प्रौद्योगिकी संस्थान भुवनेश्वर/Indian Institute of Technology Bhubaneswar
जटनी - 752050/Jatni–752050,**खोर्धा/** Khordha,**ओड़िशा**, **भारत/** Odisha, India

CERTIFICATE

It is certified that the project work titled "**Ultrasonic vibration assisted Electro-jet machining for micro-milling/grooving applications of metal sheets/foils**" is a Bonafede work of **D Krishna Vamsi** (Roll No:17ME02028), carried out under my supervision in partial fulfilment of the requirement for the award of degree of B.Tech. in Mechanical Engineering and M. Tech in Manufacturing Engineering, in School of Mechanical Sciences, Indian Institute of Technology Bhubaneswar.

The reported work is carried out during the academic year 2021-2022 and has not been submitted elsewhere for a degree.

Date:

Dr. Suvradip Mullick
Assistant Professor
School of Mechanical Sciences
Indian Institute of Technology Bhubaneswar
Bhubaneswar, 752050, Odisha, India

ACKNOWLEDGEMENTS

I am profoundly grateful to my supervisors, Dr. Suvradip Mullick for his continuous guidance and support during this work. He has always inspired me through our technical and general discussion to do my work on time to properly understand fundamentals. I am thankful to him for their guidance, support, and inspiration, which helped me make the right decisions. I never had a tough time in spite of the COVID-19 pandemic period. It was solely due to the kind and patient guidance of my supervisor. He has always stood by me in tough times and are always ready with prompt help and encouragement. He could really lift up my spirit sky high. Therefore, this report is well incomplete without expressing special thanks and gratitude to him.

I would like to express my deepest appreciation to Dr. Mihir Kumar Pandit, Head of the school of mechanical sciences, for all the encouragements. I thank all my teachers for their contribution to my studies and research work. They have been great sources of inspiration.

I express my sincere thanks to all faculty members and staff of the School of Mechanical Sciences, IIT Bhubaneswar, for their constructive suggestions and constant encouragement. Last but not the least I owe my sincere thanks to all those who helped me in many tangible and intangible ways.

D Krishna Vamsi
17ME02028

DECLARATION

I certify that,

1. The work contained in this thesis is original and has been done by me under the guidance and supervision of Dr. Suvradip Mullick.
2. The work has not been submitted to any other institute for any Degree or Diploma.
3. I have followed the guidelines stipulated by the institute in preparing the Thesis.
4. I have conformed to the norms and guidelines given in the Ethical Code of Conduct of the institute.
5. Whenever I have used materials (data, theoretical analysis and text) from other sources, I have given due credit to them by citing them in the text of the thesis and giving their details in the References.

D Krishna Vamsi
17ME02028

Ultrasonic vibration assisted Electro-jet machining for macro to micro grooving applications of thin metal sheets/foils

Abstract

Electrochemical machining (ECM) is a non-conventional machining process, where machining can be done without the development of any residual stresses and thermal damages, further the process is free from dross or burrs. The issue with ECM is mainly choosing the proper working parameters in order to obtain high degree of accuracy under good surface conditions. In this work, an electro-jet machining system is used for drilling in thin sheets of aluminium and Inconel, where the electrolyte is used as a jet from anozzle concentrically to the electrode (metal wire). Electro-jet machining (EJM) canenhance control of electrolyte flow and thus can be used for micro-fabrication and micro-patterns generation for the development of high precision manufacturing components, structured surface, etc. This project is particularly focused on investigation on the drilling performance under the application of pulsed DC current and ultrasonic vibration to the work-piece to produce macro to micro-holes. MRR for micro milling/grooving applications on metal sheets/foils effect of ultrasonic vibration on MRR in electro jet micro machining for micro milling applications. Further, a detailed investigation on the effects of process parameters (pulse frequency, duty cycle and ultrasonic vibration frequency) has been carried out for obtaining optimum drill quality having minimum hole diameter and overcut along with maximum material removal rate (MRR).

Keywords: Electro-jet machining, Ultrasonic vibrations, Pulsed mode, Overcut, MRR

CONTENTS

Contents **Page No.**

LIST OF FIGURES

Fig. No.: Caption Page No.

LIST OF TABLES

CHAPTER 1:
INTRODUCTION

1.1 Theoretical Background

The electrochemical machining (ECM) technique can be used to make complex-shaped components in a variety of industries, including automotive, forging dies, electric, and surgical components. Because of its low machining accuracy and difficulty in tool design and electrolyte disposal, ECM has yet to become a widely used technique.

Turning cylinders to create extremely smooth surfaces is one of the most common applications of ECM in the automobile industry. To smooth uneven surfaces, the industry has used a variety of standard and non-traditional procedures. Abrasive cutting procedures including grinding, lapping, and burnishing are common in mechanical methods, although non-conventional methods like ultrasonic machining and abrasive flow deburring use alternative mechanisms. The ECM method is being extended from die sinking to turning in order to achieve high precision and surface polish in straight and form turning of difficult-to-machine materials with a high slenderness ratio. Many turning activities in conventional and copying lathes will be simplified, and grinding operations will be eliminated. Electrochemical turning has recently acquired popularity as a finishing technique. Axially symmetric turned pieces can be produced by feeding a shaped tool into a spinning workpiece. Large symmetric workpieces can be created with little tools in this manner. Electrochemical turning can also be used to machine thin-section turned items that would be difficult to machine otherwise due to the distorting effect of cutting forces.

1.2 Electrochemical machining

Metal is removed in electrochemical machining (ECM) using an anodic dissolving process based on Faraday's equation of electrolysis. It's an electrochemical machining process that's not as common as regular machining. The tool is connected to the cathode, or negative, terminal of the DC power supply, while the workpiece is attached to the anode, or positive, terminal. The material from the anode is removed. ECM is capable of machining extremely hard or difficult-to-machine materials. ECM can only manufacture electrically conductive materials. The method can machine or cut complicated curves or cavities in hardened steels such as titanium, Carbide, and other materials. Electrochemical machining can be used to machine both external and internal geometries.

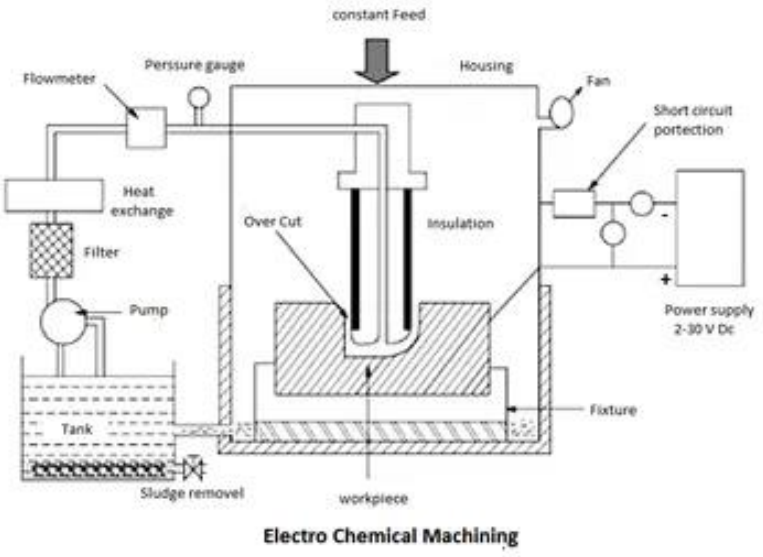

Fig.1: Schematic of Electro Chemical Machining Setup [1]

1.2.1 Types of electrochemical machining

Immersion type ECM: The tool and workpiece are both submerged in the electrolyte during electro chemical milling. For EC milling, the movement of the tool electrode is monitored here. Acid electrolytes are often used in EC immersion milling to minimise flocculation and reduce processing effect; however, they are not ecologically friendly, and they require extensive equipment maintenance if employed.

External jet type ECM: We employ an exterior nozzle in external jet EC milling to manufacture workpieces using a solid electrode as a tool cathode. When opposed to the Immersion kind, this procedure is faster. Due to external fluid supply, it is difficult to deliver fluid in the machining gap as the milling depth increases.

Internal jet type ECM: In this method, we employ a cathode tube for the electrode, and electrolyte flows through the inner tube at a very high velocity into the cutting site. The electrode's internal jet has the features of a high electrolyte flow rate and a robust mass transfer mechanism

1.2.2 Working principle of ECM

Like ECM, also works on the principles of electrolysis. In ECM workpiece atoms are removed by the electrochemical dissolution method.

Principle of electrolysis: "When electric current flows between the two electrodes, electrolysis occurs. The entire electrode and electrolyte system is called an electrolytic cell. The chemical reactions at the anode are called anodic dissolution. We can calculate the amount of material removed using Faraday's laws".

From Faraday's laws of electrolysis, which state that

- ❖ 1st law: "The amount of material deposited or removed is directly proportional to the amount of charge (flow of current) applied through an electrolyte."
- m ∝ Q
- ❖ 2nd law: "when same amount of charge is passed through several electrolytes, the mass of the substance removed or deposited are proportional to their respective chemical equivalent or equivalent weight."
- m ∝ ECE (∈)
- m ∝ Atomic Weight/$Valency$

Where,
- m → mass of the material removed.
- I → current, A
- t → machining time, min
- E → chemical equivalent weight, gm. (E =aZ)
- a → atomic weight
- Z → valency
- F → faraday's constant (F=96500 coulombs)

$$m = \frac{ItE}{z} \qquad [1.1]$$

At the anode and cathode, numerous different reactions can be initiated by applying a voltage difference between the electrodes. Figure 2 shows the solubility of iron in a water solution containing sodium chloride (NaCl) as an electrolyte.

The result of electrolyte dissociation leads to

$$H_2O \rightarrow H+ + OH-$$
$$NaCl \rightarrow Na+ + Cl-$$

The positively charged cations of H^+ and Na^+ are directed to the cathode as the cathode is connected to the negative terminal.

"At the anode, Fe changes to Fe^{++} by losing two electrons."

$$Fe \rightarrow Fe++ + 2e-$$

"At the cathode, the reaction involves the generation of hydrogen gas and hydroxyl ions."

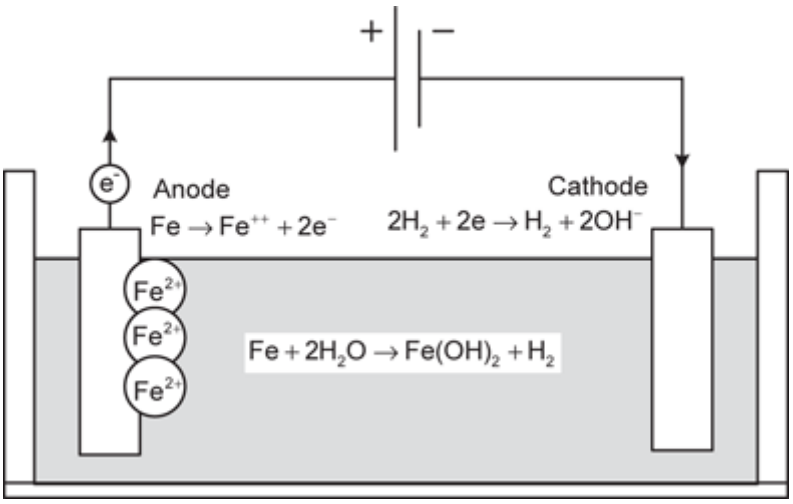

Fig.2: Electrochemical reactions during ECM of iron [2]

$$2H_2O + 2e^- \rightarrow H_2 + 2(OH)^-$$

These EC reactions cause iron ions to interact with other ions and precipitate out as iron hydroxide, Fe (OH)2.

$$Fe + 2H_2O \rightarrow Fe(OH)_2 + H_2$$

The ferrous hydroxide can react with oxygen and water to form ferric hydroxide, Fe (OH)2.

$$4\,Fe(OH)_2 + 2\,H_2O + O_2 \rightarrow 4\,Fe(OH)_3.$$

Electrolysis is the dissolution of iron at the anode and the creation of hydrogen at the cathode using this combination of metal electrolytes. Iron produces an insoluble precipitate. The anode dissolves and forms on the cathode as a result of this combination of metal electrode and electrolyte, leaving the cathode's structure unaltered. To enhance mass and charge transfer through the sublayer near the anode, the electrolyte is driven through the inter-electrode gap at high speed. The electrolyte cleans the inter-electrode gap of breakdown products such metal hydroxides, heat, and gas bubbles. The electrodes and electrolyte used in the ECM must be selected so that deposition cannot occur on either electrode.

1.2.3 Typical ECM process parameters

a. Supply voltage (V)	-	5 to 30 Volts.
b. Current (I)	-	50 to 5000 A.
c. Electrode gap	-	0.1 mm to 0.2 mm.
d. Tool material	-	Copper (Cu), Brass, or Steel.
e. Tool feed rate	-	0.5 mm/min to 15 mm/min.
f. MRR	-	1600 $mm3$/min per 1000 A.
g. Surface finish	-	0.1 μm to 0.5 μm

h. Specific Power Consumption - 7 W/mm3/ min

1.2.4 Applications of ECM

ECM's benefits are fully used in the manufacturing of turbine blades, which include its applicability regardless of material hardness for creating complicated geometry, good surface quality with stress- and burr-free surfaces, and cost-effective large-scale production. ECM is a key component of a highly integrated turbine blade manufacturing system that comprises broaching, EDM, automated deburring, and proprietary 360-degree ECM, which produces the air foil, platform, leading, and trailing edges to very high precision in a single operation. Blades may be manufactured inexpensively in batches of fewer than 2000 due to a considerable decrease in total production lead time due to a highly automated system. The use of ECM in the machining of integrated bladed rotors and turbine wheels has proved critical. The blades were machined individually before being joined on the drum. The component may now be manufactured in a single operation at a reduced cost and with better quality control by switching to ECM. The items' performance efficiency increased as the quality improved. ECM also creates various components in the aerospace and aviation sectors that are more efficient than traditional machining, such as rocket engine parts and jet engine rings. For drilling tiny, deep holes, a highly specialised modification of ECM called as shaped-tube electrolytic machining (STEM) is employed. A hollow titanium tube is covered with an electrically insulating chemically resistant resin in this method. To ensure precise penetration, the electrodes are routed via a guiding system. The electrolyte is pumped through the tube's centre. This technology has been used to drill holes with sizes ranging from 0.5 to 3.0 mm with a depth-to-diameter ratio of up to 300:1. The majority of STEM's current industrial uses include drilling in difficult-to-cut superalloys, such as cooling holes in turbine blades. ECM offers a wide range of applications in numerous sectors, including mould, car, medical, and defence. Artificial hip joints made of titanium and cobalt alloys, as well as valve components, are now well-established industrial procedures.

1.2.5 Advantages and Disadvantages

Advantages

- Negligible tool wear.

- Complex and concave curvature parts can be produced easily by the use of convex and concave tools.
- No forces and residual stress are produced, because there is no direct contact between tool and workpiece.
- An excellent surface finish is produced.
- Less heat is generated.

Disadvantages

- The risk of corrosion for tool, w/p and equipment increases in the case of saline and acidic electrolyte.
- Electrochemical machining is capable of machining electrically conductive materials only.
- High power consumption.
- High initial investment cost.

CHAPTER 2:
LITERATURE REVIEW

2.1 Literature Review

This chapter presents the literature review of papers presenting ECM and EJM

2.1.1 State of the art

Zhang et al. proposed a novel combined process for the EC milling of a DNG in a single milling pass. The process begins using a tube electrode without insulation for the EC drilling of a blind hole; following this, EC milling is performed by changing the feed direction of the tube tool from the Z direction to the milling path in the X–Y direction. Simulation and experimental observations have investigated the distribution of the electrolyte flow field during machining and analyses how the electrolyte flow status affects the machining process. [4]

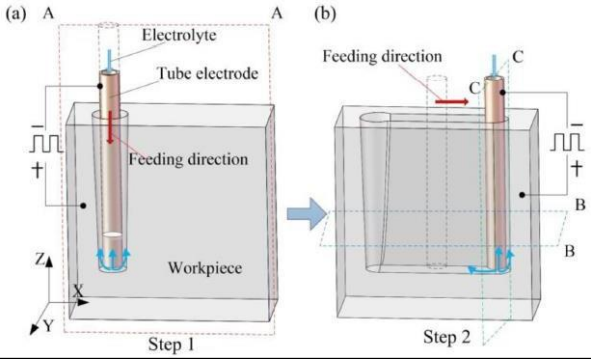

Fig.3. Schematic of electrochemical milling of a deep narrow groove with a tube electrode. [4]

Hung et al. used jet-ECM with mixed gas to improve the surface accuracy of grooves. Combined with the process characteristics, they concluded that jet-ECM is usually employed to fabricate micro-grooves no deeper than 1 mm; this is because the bottom end of the tube electrode is used to mill groove, and it is difficult to go any deeper because the electrolyte jetting from the nozzle then becomes uncontrollable. [5]

Kawanaka et al. developed a method for selective surface texturing using electrolyte jet machining. This process is characterized by the ability to control the surface finish of the removed or added micro patterns by the current density in the electrolyte jet. From the result, higher current density leads to a mirror-like surface finish, while lower current density realizes significantly rough and complicated structures. [6]

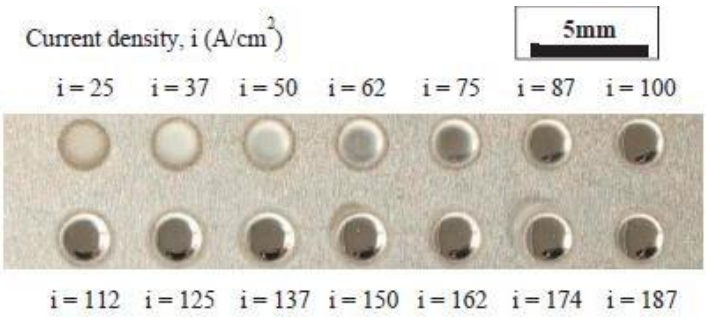

Fig.4. Dimples machined with increasing current densities [6]

Ming et al. developed a jet electrolytic machining process to improve anodic dissolution localization by submerging both the nozzle and the workpiece in the kerosene, and verification experiments are conducted by fabricating micro-dimples. Kerosene submerged Jet-ECM process shows a better localization if appropriate voltages are chosen. [7]

Uttarwar et al. studied the effect of voltage variation on MRR for ECM of Stainless steel. With the gradual increase in voltage, MRR increases while the Inter Electrode gap is maintained constant during the whole experimentation. [8]

Burger et al. worked on ECM characteristics and resulting surface quality of Nickel base single crystalline material LEK94. It says current density was found to be the major machining parameter affecting the surface quality of LEK94 & current density beyond 1A/mm^2 yields more homogeneous dissolution rates, which leads to a very good surface finish. [9]

2.1.1 Effect of pulse DC in ECM process

Kozak et al. developed a pulse electrochemical micromachining (ECMM) process for generating complex micro-components of high accuracy. Analytical model was developed to analyze the effect of voltage and feed rate on process performance. From the result, a higher frequency (1 MHz) indicated smaller side and frontal gaps with sharper edges than the results at 250 kHz. [10]

Mithu et al. investigated the effect of applied frequency pulses on the shape and size of the fabricated micro holes, machining time, and material removal rate for various types of micro tools. Short pulse-on voltage with long pulse-off time is preferred in order to improve accuracy and surface finish as it improves the localization of dissolution to sub-micrometer. [11]

2.1.1 Effect of tool vibration in the ECM process

Heiwdy et al. investigated the effect of tool vibration on the material removal rate in ECM. The analytical model suggests that with an increase of vibration amplitude, frontal gap size decreases, which leads to an increase in the current density, so ultimately, MRR increases. In tool vibration case sparking and tool damage can occur, so in order to avoid it, feed rate has to be restricted. [12]

Rusraz et al. investigated the effects of ultrasonic vibration of the electrode on surface finish in the electrochemical micromachining process. As from the results ultrasonic vibrations help to decrease the surface roughness parameter *R*a in comparison to the classical electrochemical process. [13]

Zagorui et al. investigated the effect of ultrasonic vibration frequency on various process parameters, i.e., current, voltage, and electrolyte temperature in the ECM process and the favorable effect of the ultrasonic field in electrochemical de-passivation in order to improve the performance of the electrochemical machining process was analyzed. [14]

2.1.5. Fabricating microgrooves by jet ECM

Wang et al. modified jet-ECM to fabricate deeper grooves for milling micro-grooves using a tube electrode with an insulating layer and to adjust the jet shape to reduce stray corrosion at the micro-groove edge. With multiple milling passes, a blind groove with a width of 1.5mm and a depth of 1.2mm was generated. [15]

Bhattacharya et al. Investigated into micro-milling of microgrooves on titanium alloy by electrochemical micromachining & concludes that by increasing machining voltage, width overcut & length overcut increases and by increasing pulse frequency width overcut and length overcut can be decreased. [16]

Ghoshal et al. discussed the influence of different electrodes on the sidewall taper of groove and found that the inverted cone electrode could effectively reduce the sidewall forming taper and improve the groove processing accuracy. [17]

2.1.6 Effects of various process parameters on MRR and surface quality in ECM

Spideal et al. studied the effects of various electrolytes for establishing more stable machining and controlled removal of the passivating layer in titanium substrates. Surface finish, MRR and pit formations using solutions of sodium halides (bromide, chloride, and fluoride, respectively) are compared with those obtained using the more commonly used sodium nitrate solution. Chloride-based electrolytes resulted in the greatest pit depths, material removal rates, and surface finish, whereas bromide based electrolytes led to greater precision. [18]

Hinduja et al. did an experiment in electrochemical milling with varying parameters like the voltage, feed rate, no. of tool passes, the shape of the electrode, and they found that the increase in feed rate decreased the depth of cut and width. Also, with an increase in voltage, depth of cut & width increased. They observed that the width and depth of the slots machined by the cylindrical tool are smaller than those machined by the square tool. [19]

Bhattacharyya et al. Observed that with a lower concentration, higher voltage, and a moderate value for the pulse-on time machining accuracy can be improved with a moderate MRR. [20]

Chen et al. investigated the influence of process parameters like voltage, pulse on time and pulse frequency and electrolyte flow etc. on the machining performance, such as material removal rate (MRR) and accuracy on microgroove machining by micro ECM. From the observation voltage and pulse on time has an impact on corner radius and the taper between the sidewall of a groove. Double nozzle was proposed to minimize geometrical deviations like corner radius and the taper of the sidewall of a groove. For better geometrical accuracy, a pulse with low voltage and short pulse on-time was preferred. [21]

Qu et al. developed a pulsating electrolyte supply system in ECM and analyzed how pulsating electrolyte affects surface roughness and MRR on Ti6Al4V sample. They observed that lower

surface roughness and higher material removal rate could be obtained by using a pulsating electrolyte with proper pulsating frequency and amplitude. [22]

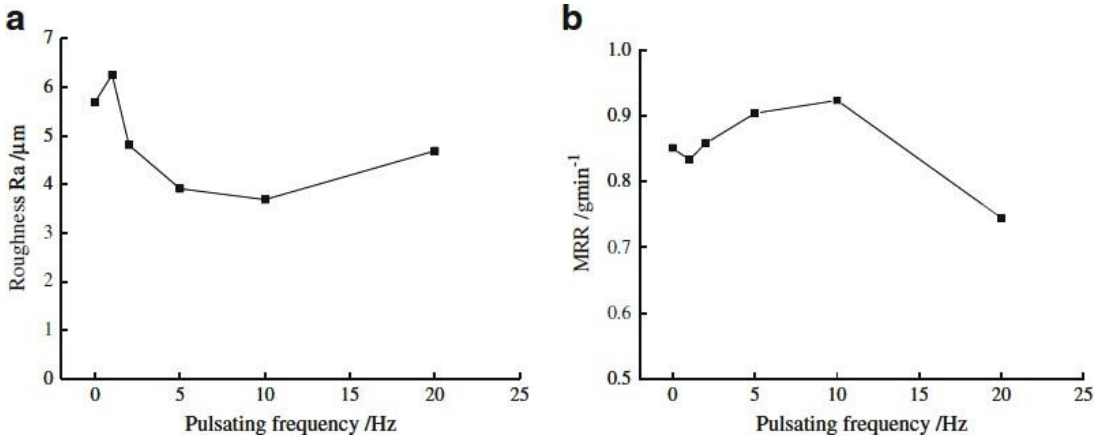

Fig.9. Effects of pulse frequency on (a) surface roughness (b) MRR. [16]

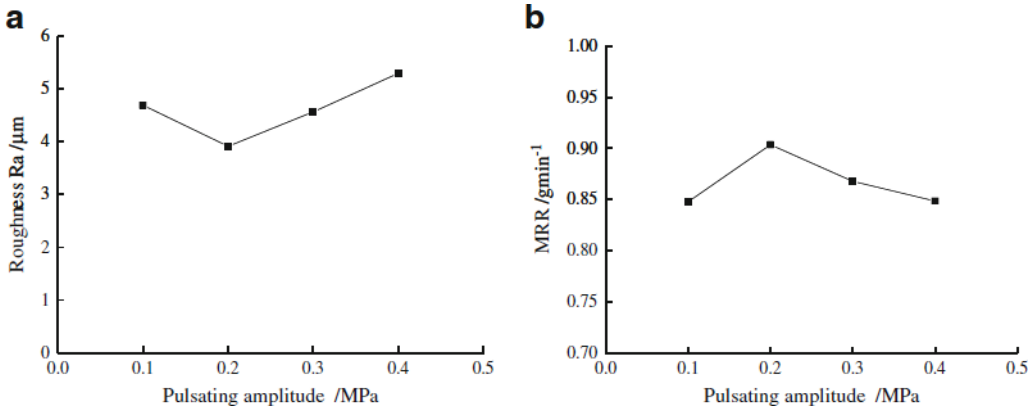

Fig.5. Effects of pulsating amplitude on (a) surface roughness (b) MRR. [16]

Goel et al. The experiments were conducted to obtain second order model using Central composite rotatable design (CCRD). A detailed experimental study of the newly developed process has been carried out. Effects of process parameters like voltage, inter-electrode gap, electrolyte concentration, electrolyte pressure and pulse on time of ultrasonic vibrations have been studied on process responses, namely, MRR and hole taper. From the results obtained after experimentation, it was observed that MRR improved with a rise in pulse on time of ultrasonic vibrations whereas the hole taper decreased with the rise in pulse on time. It was concluded that combining ultrasonic vibrations with the Jet-ECMD resulted in an enhancement of the process capabilities in terms of improvement of MRR and reduction in the hole taper.

2.2 Objective Formulation

- To formulate analytical model towards calculation of MRR and overcut in ultrasonic assisted electro jet drilling, by giving ultrasonic vibrations to the workpiece and feed rate to the tool.
- To investigate the effect of pulsed power supply and application of ultrasonic vibrations in Electro-jet drilling.
- To study the effect of the process parameters like pulse frequency, Duty cycle, and Ultrasonic vibration frequency on machining performance (MRR, hole diameter and overcut)
- To optimize the process using Response surface methodology.

2.3 Methodology/ Work Plan

- Design and development of EJMM with pulse power supply system by connecting pulse generator with the existing EJMM set-up.
- To assemble all the equipment like pulse generator and ultrasonic transducer with the existing EJMM setup.
- Process demonstration & to carry out detailed experimentation to study the effect of process parameters on cut quality in EJMM.
- Finding optimum process condition where cut quality have been checking through optical microscope.
- Optimising the model by using Design of Experiments.

CHAPTER 3:
FORMULATION OF ANALYTICAL MODEL

ECM is based on Faraday's law of electrolysis. Which is comprised of two laws.

- ✓ 1st law: Amount of material deposited or removed is directly proportional to the amount of charge (flow of current) applied through an electrolyte.

$$W \propto Q$$

- ✓ 2nd law: When the same amount of current is passed through several electrolytes, the mass of the substance removed or deposited are proportional to their respective chemical equivalent or equivalent weight.

$$W \propto ECE$$

$$W \propto \text{Atomic Weight}/\ Valency$$

Table. 1. NOMENCLATURE

E: Electro chemical equivalence (a / z)	*k*: Electrolyte conductivity (*k* = 1/r)
W: Mass of material removed	r: Resistivity
Q: Charge applied	η: Machining efficiency
V_m: Volume of material removed	*F:* Faraday's constant (96,500 C)
I: Current	ρ_m: Density of work piece material (g/mm3)
V_0: Applied potential	*a*: Vibration amplitude (mm)
A: Machined area	ω: Angular velocity (rad/s) = 2πf
a : Atomic weight	f: Vibration frequency (Hz)
z: Valency	t: Time (sec)
h: Equilibrium gap (mm)	ϕ: Phase angle (rad)
C: Constant *E:* Electrochemical equivalent	

So, $W = \frac{Qa}{z}$

$\Rightarrow W = \frac{Ita}{Fz}$

$\Rightarrow \rho_m V_m = \frac{Ita}{Fz}$

As we know, MRR= (Vm/ t) = $\frac{Ia}{\rho_m F z} = \frac{IE}{\rho_m F}$ where E = a/z

Volumetric MRR = $\frac{IE\eta}{\rho_m F}$

Mass MRR = $\frac{IE\eta}{F}$ [3.1]

3.1 MRR of EJMM under normal conditions:

When there is continuous DC, the amount of material removed during µECM can be determined by combining Faraday's first law and Ohm's law which can be stated as:

As MRR in ECM = $\frac{V_0 E}{RF\eta\rho_m} = \frac{V_0 E}{\frac{rh}{A}F\eta\rho_m} = \frac{V_0 EA}{Frh\eta\rho_m}$

MRR under continuous DC = $\frac{V_0 EA}{Frh\eta\rho}$ [3.2]

3.1.1 MRR under continuous DC current:

When continuous DC is present, the quantity of material lost during ECM may be calculated by combining Faraday's first law and Ohm's law, which can be written as:

As MRR in ECM = $\frac{V_0 E}{RF\eta\rho_m} = \frac{V_0 E}{\frac{rh}{A}F\eta\rho_m} = \frac{V_0 EA}{Frh\eta\rho_m}$ [3.3]

MRR under continuous DC = $\frac{V_0 EA}{Frh\eta\rho_m}$ [3.4]

3.1.2 MRR under pulsed DC current [17]:

Again, MRR can also be written as = $\frac{V_m}{t}$,

$$Vm = \frac{EV_0 At}{Frh\eta\rho_m} \quad [3.5]$$

When using pulsed ECM, the material removal for each pulse is believed to occur only during the fraction of t_{on} time when faradaic current is flowing. Every pulse will result in the charging and discharging of the double layer.

Given that material removal occurs exclusively during all pulse-on time durations, the volume of material removed ($V_{m\text{-}on}$-time) may be calculated by integrating tonne time.

$$\Rightarrow Vmon\text{-}time = \int_{t*}^{t_{on}} \frac{EV_0 A}{Frh\eta\rho_m} dt \quad [3.6]$$

Because material removal occurs only while faradaic currents are present, t* is the start time of the flat voltage.

Where, tp is time period of one pulse

δt is called duty cycle in %,

γ^* is the percentage of pulse-on time to start almost flat voltage

f is the applied frequency in hertz.

MRR = $Vmon{-}time/\ ton + toff = Vmon{-}time/\ tp$

$$\text{MRR in case of pulse DC} = \frac{EAV_0(1-\gamma^*)\delta_t}{Frh\eta\rho_m} \quad [3.7]$$

Neglecting γ^* in the experimental conditions

$$\text{MRR in case of pulse DC} = \frac{EAV_0\delta_t}{Frh\eta\rho_m} \quad [3.8]$$

3.2 MRR under ultrasonic vibration in EJMM:

- Displacement equation of tool due to vibration is:
- X (t) = a sin (ω t + ϕ) where ω = 2Πf

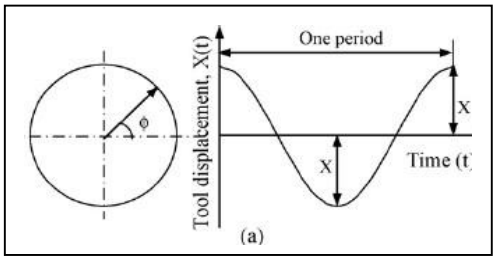

Fig.6. Displacement-time graph for tool vibration [2]

- The velocity of tool at any time due to tool vibration is:
- $\dot{X}(t) = a\ \omega \cos(\omega t + \phi)$

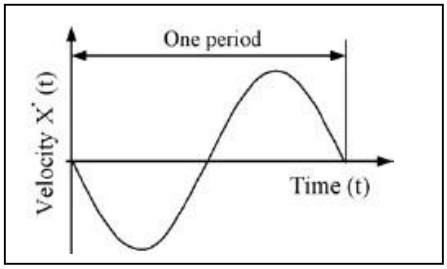

Fig.7. Velocity-time graph for tool vibration [2]

- In ECM assisted by ultrasonic assisted vibration,
- The instantaneous tool feed rate is given by the equation-

- (f_v) = f ± $\dot{X}$(t)
- (f_v) = f ± a ω cos (ω t + ϕ) (f is the initial feed rate)

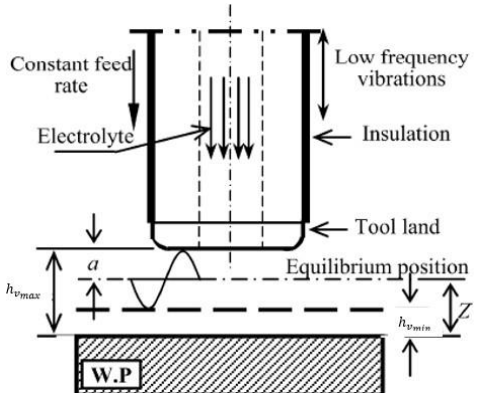

Fig.8. Tool–work piece configuration during ECM with tool vibration. [2]

- In case of EJMM assisted with ultrasonic vibration, the frontal gap will be changed because of the variation in the tool displacement.
- So, the frontal gap due to vibration will be h_v= Z ± a sin (ω t + ϕ)
- Z is the equilibrium position of the tool = h_e− a.

- The maximum value of frontal gap (h_v) max is obtained at the maximum value of a sin (ω t + ϕ).
- Which is ensured by increasing amplitude value (a) and the angular velocity at sin (ω t + ϕ) =1.

- Maximum value of frontal gap (h_v) max = Z + a = h_e
- Minimum value of frontal gap (h_v) min = Z – a = h_e – 2a

- The material removal rate (MRR) in ECM is given by the equation-
    - MRR= (Vm/ t) = (I a)/(ρmFz) = (I E)/(ρmF), (where E = a/z)

- Volumetric MRR = (I E)/($\eta\rho mF$)

- MRR = ($k\ Vo\ E\ A$) / ($hv\ \eta\ \rho m$F)

- By using the equation h_v= Z ± a sin (ω t + ϕ)
- MRR due to ultrasonic vibration ($MRRV$) = ($k\ Vo\ E\ A\ \eta$) / (ρmF [Z ± a sin (ω t + ϕ)])

- At ($hvmin$), MRR will be maximum,
- MRR$vmax$ = (k ($Vo - \Delta V$) $E\ A$) / ($\eta\ \rho mF$ ($he - 2a$))
- At (hvmax), MRR will be m,
- MRR$v$min = (k ($Vo - \Delta V$) $E\ A$) / ($\eta\ \rho mF$ (he))

3.3 MRR under ultrasonic vibrations and tool feed rate in EJMM

- In the above equation of MRR, if the inter electrode gap can be maintained constant by giving a constant feed rate to the workpiece.
- Then the equation of MRR can be modified as
- ($MRRV$) = ($k\ Vo\ E\ A\ \eta$) / (ρmF [hc ± a sin (ω t + ϕ)])
- hc = (Vo Mx) / (ρmFr)
- Here, hc is the initial gap between the electrode and the workpiece, it will be maintained constant by giving the required feed rate ‘s’, which needs to be calculated.

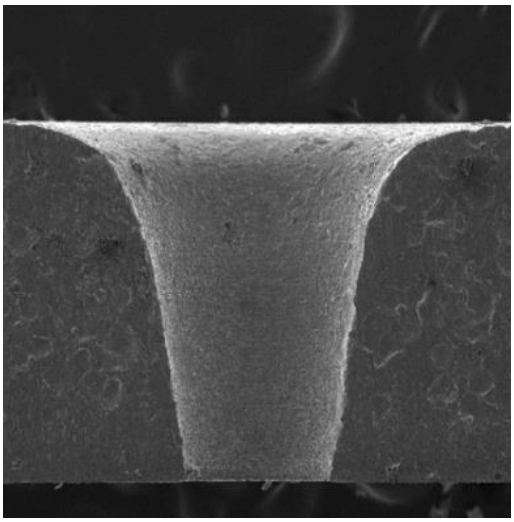

Fig.9. overcut in drilled holes by EJMM [1]

- In the above equations, the overcut was not considered,

- To calculate the overcut, the following equations are derived.

- Let, MRR be the material removal rate, at be the area of cross-section and dx be the depth of the hole that needs to be cut.

- So, MRR= Area of cross-section x depth of hole, => dx = MRR / π/4 $(dt)^2$
- But here the hole is not cylindrical, because of overcut, we get an approximate shape of a frustum of cone.

- Actual dx = MRR / $\frac{\pi}{4}(\mathrm{dt} + \mathrm{Overcut})^2$
- Actual dx = MRR / $\frac{\pi}{4}(\mathrm{dt} + (\mathrm{Overcut\ Top} + \mathrm{Overcut\ Bottom})/2)^2$
- Here, MRR = $(k\ Vo\ E\ A\ \eta)$ / $(\rho mF$ [hc ± a sin (ω t + ϕ)]),
- hc = $(Vo$ Mx) / $(\rho mF$r)
- Actual dx = $(k\ Vo\ E\ A\ \eta)$ / $(\rho mF$ [hc ± a sin (ω t + ϕ)]) / $\frac{\pi}{4}(\mathrm{dt} + (\mathrm{Overcut\ Top} + \mathrm{Overcut\ Bottom})/2)^2$

3.4 Validation of mathematical model with experimental result for MRR without the application of Ultrasonic vibration:

Process parameters values used in the experiments are:
Workpiece used as aluminium sheet of 500 μm thickness, atomic weight (a) is 27, valency (z) is 3, F=96500C, IEG (h)= 0.2 mm, supply pulse voltage V_0= 20V, density of aluminium (ρ)= 2.71 mg/ mm^3, density of Inconel625 (ρ)= 8.43 mg/ mm^3, conductivity of electrolyte ($\boldsymbol{k}$) = of 0.02 V/A mm [Ref.12], duty cycle (δ_t)= 80% or 0.8.

For the pulse DC condition MRR equation is: $\dfrac{\boldsymbol{E\ A\ V_0\ \delta_t}}{\boldsymbol{\rho\ F\ r\ h}}$

For 40%, 60%, 80% duty cycle and at 0.5, 5 & 50 kHz pulse frequency from the mathematical model equation MRR was obtained as 0.98 mg/min, whereas the value obtained was 0.27 mg/min from the experiment. So, the experimental value is nearly 0.2times of predicted model.

Some of the reasons for these variations are that the model equation pulse frequency parameter was not considered, but as from the graphs, pulse frequency also impacts MRR. So, during the pulse DC power supply, there may be some delay before starting an anodic solution, so the MRRwas lower in the experimental value.

Table. Comparing the Experimental and theoretical change in MRR for Aluminum and Inconel.

Pulse Frequency	Duty Cycle	Experimental MRR (Al)	Experimental MRR (Inconel)	Experimental % change	Theoretical% change
0.5	80	0.271	0.246	9.2	8.6
0.5	60	0.246	0.224	8.1	7.5
50	40	0.191	0.176	7.8	8.2
50	60	0.212	0.197	7.1	7.6

CHAPTER 4:
EXPERIMENTAL DETAILS AND RESULTS

In this section let us discuss the experimental setup that will be us. Ultrasonic vibrations will be introduced to get better surface finish and less overcut. A setup will be developed to give feed rate to the workpiece along with ultrasonic vibrations, this can be achieved by using ultrasonic transducers and Ultrasonic generators.

4.1 Experimental Setup Description:

The whole EJMM setup can be categorized in four sub-systems: Power supply system, Electrolyte circulation system, Tool assembly.

In addition to develop EJMM assisted with ultrasonic vibration two more sub systems are added with respect to EJMM setup: Ultrasonic transducers and Ultrasonic vibration generator. The experiment was performed on ECM setup and Ultrasonic vibrations were given to the workpiece by placing the workpiece holder on the Stainless-steel box.

A setup is arranged to give ultrasonic vibrations to the workpiece, this can be achieved by using ultrasonic transducers and generator setup.

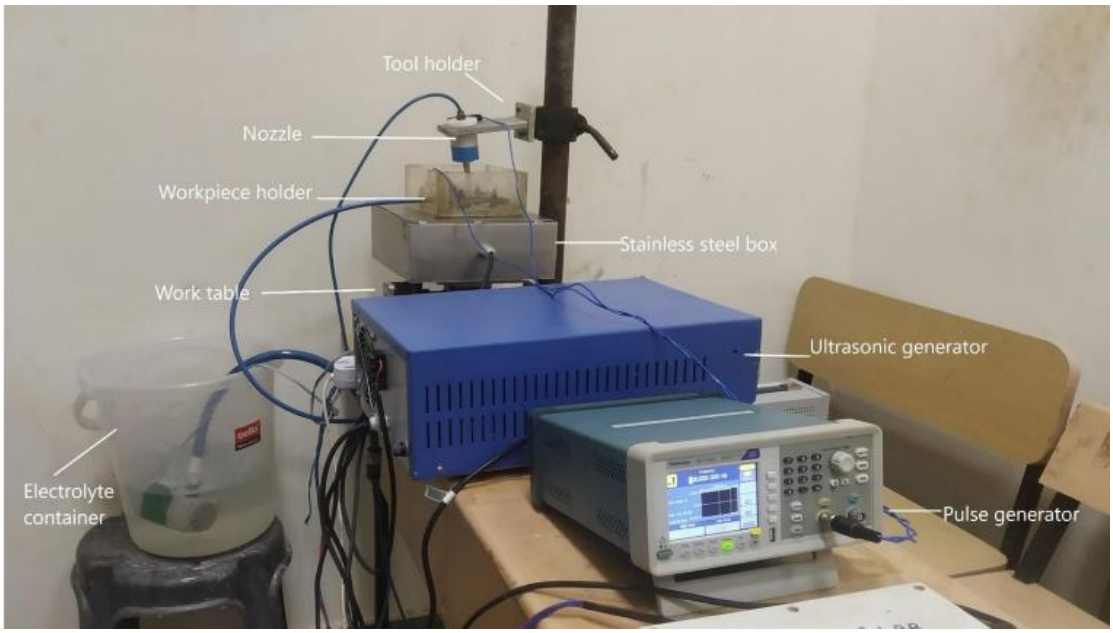

Fig10: Complete Setup

Ultrasonic vibration setup:

Ultrasonic generator was used for generating vibration in the transducers which were placed in a stainless-steel box. Here the frequency range of ultrasonic generator lies between 25-35 kHz. Hereinput power supply was given as AC power supply.

Fig.11. ultrasonic generator

Fig.12. transducers mounted inside SS box

Frequency of vibration was controlled by ultrasonic generator. Here in this setup four ultrasonic transducers are placed inside a stainless-steel box and on the top of the stainless-steel box machining tank was placed on which aluminum workpiece was mounted with the help of workpiece holder as shown in the Fig.18. So, by applying ultrasonic vibration IEG changes so MRRimproves, and also better flushing occurs due to vibration.

The experiment is carried out in Pulsed DC mode and the experimental parameter like Voltage, inter electrode gap and the electrolyte concentration are kept constant, and the parameters like

Pulse Frequency, Duty cycle and Ultrasonic vibrations frequency is varied and the outputs MRR, Hole diameter and Overcut are measured.

Ultrasonic generator was use for getting vibrations in the transducers which were placed in a stainless-steel box. Here the frequency range of ultrasonic generator lies between 28-34 kHz. Here, the input power supply was given as AC power supply.

4.1 Experimental Observations to find the effect of process parameter on drilling.

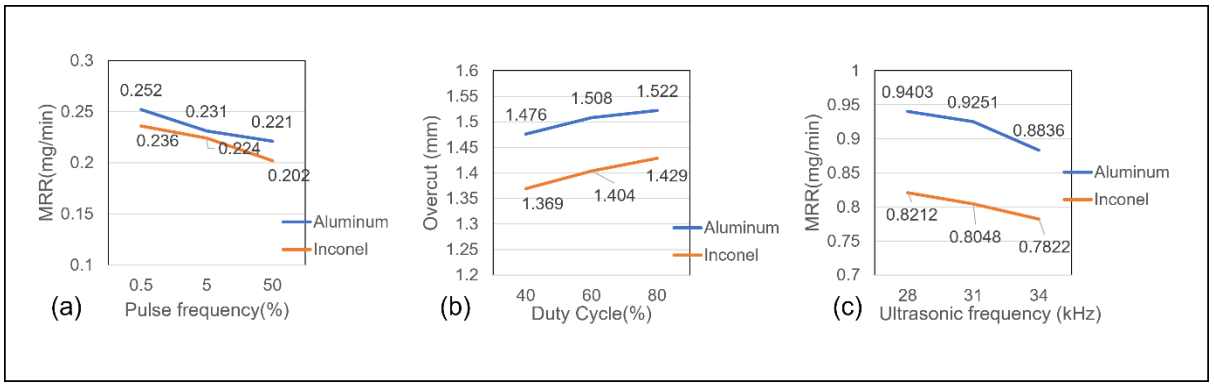

Fig 13: Effects of the individual parameters on the MRR

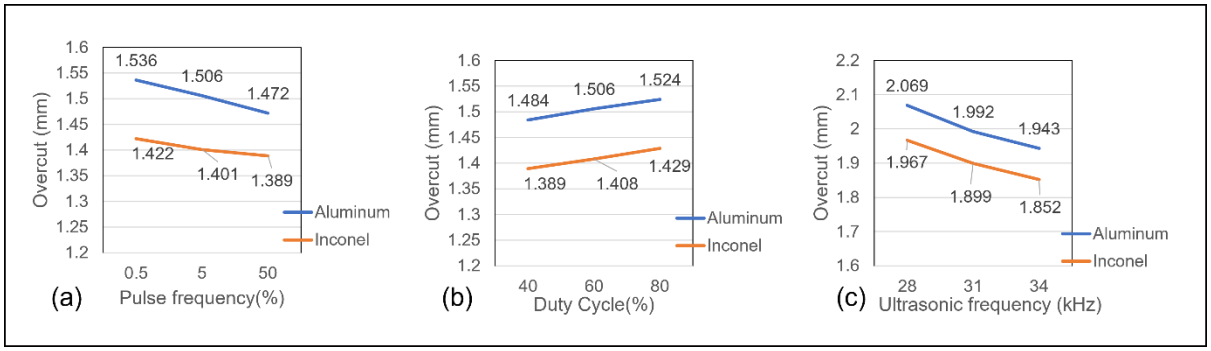

Fig14: Effect of individual parameters on Overcut

The Theoretical MRR is in the range of 1.02 to 1.17 mg/min for Aluminium sheet and in the range of 0.81 to 0.98 mg/min for Inconel sheet using the equation derived above.

The percentage of change in MRR between aluminium and Inconel sheet in Experimental MRR is 6% to 9 % and the percentage change in Theoretical MRR is 8% to 12%.

4.2 Optimization of drilling process using Response surface methodology

Optimization by Response Surface methodology was done, it involved three major steps, firstly statistically designed experiments, secondly, estimate the coefficients in a mathematical model and finally predicting the response and checking the adequacy of the model within.

Box-Behnken designs are used to generate higher order response surfaces using fewer runs than a normal factorial technique.

The experimental results have also been analyzed using analysis of variance (ANOVA). The results of ANOVA for MRR, Hole diameter and Overcut are tabulated in below table. The values of all deterministic constant (R2) for all the responses are above 90%. The term lack-of-fit is non-significant for all responses as it is desired.

For Response surface designs the perturbation plot shows how the response changes each factor moves from the chosen reference point. The lines represent the behaviors of each factor, while holding the others constant at the reference value. Design-Expert sets the reference point default at the middle of the design space (the coded zero level of each factor). In the perturbation plots, each process parameters are represented in coded units, where the low, middle and high levels of each parameter are coded as -1, 0 and +1 respectively.

Process parameters and Experimental design levels:

Table2: Levels of selected Input Variables for both the materials.

FACTORS	Units	Level 1	Level 2	Level 3
Pulse Frequency	kHz	0.5	5	50
Duty Cycle	%	40	60	80
Ultrasonic Frequency	kHz	28	31	34

The graphs showing the “predicted vs. actual plot” for all the three responses in two different materials represented in Figures below. They indicate that the predicted values are in good agreement with the experimentally measured values. Further, to verify the adequacy of model, two confirmation experiments for both aluminium and Inconel were conducted, and the measured values of responses were verified with the predicted values. The percentage errors for all responses are within reasonable limits, and also the response values are well within the 95% confidence interval (CI) and prediction interval (PI) given by the software.

Validation table

Predicted vs actual graphs for aluminum sheet-

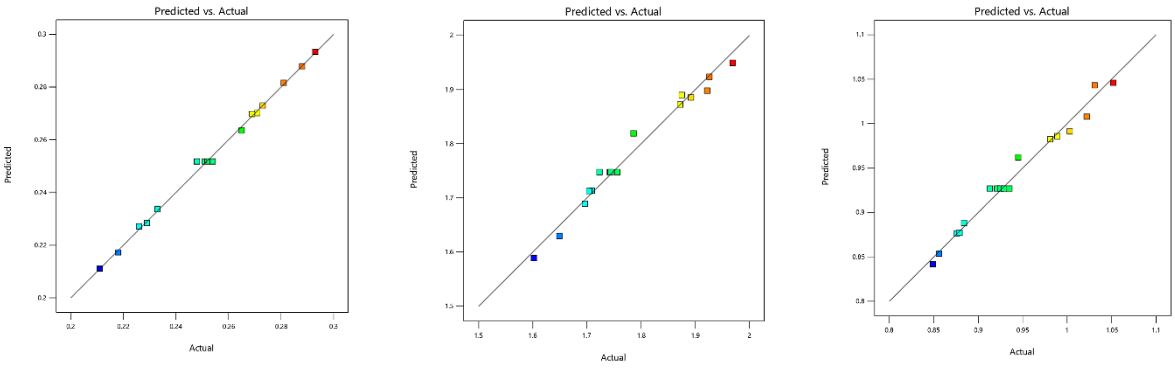

a. MRR b. Hole Diameter c. Overcut

Fig15: Aluminum sheets (Predicted vs Actual Graphs)

Predicted vs actual graphs for Inconel sheet-

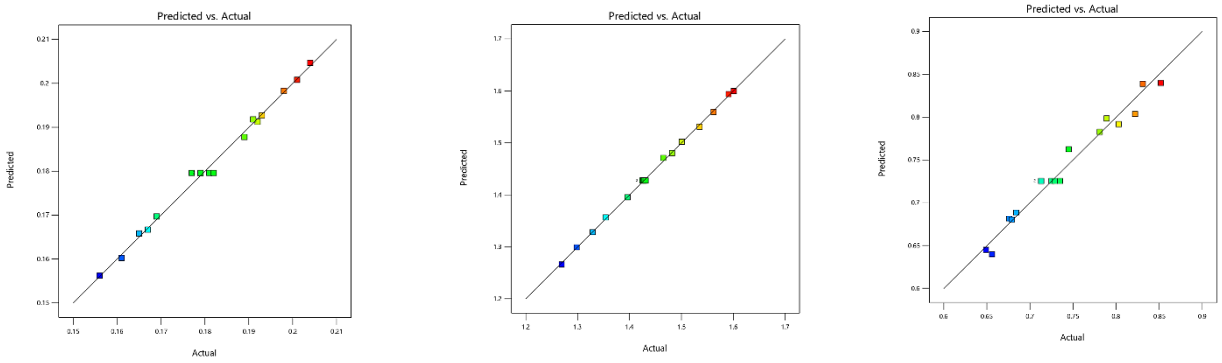

a. MRR b. Hole Diameter c. Overcut

Fig16: Inconel sheets (Predicted vs Actual Graphs

The resulting ANOVA tables for the reduced quadratic model for all three responses, for both Aluminium sheet and Inconel sheet are given in Appendix. An ANOVA table contains columns labeled "Source", "Sum of Squares", "DF-degrees of freedom", "Mean Square", "F value", and "p-value prob.4F". Model sum of square (SS-model) represents the measure of variation or deviation from the mean value, and is used for describing how well a model represents its data. The table also presents other adequacy measures, R2, Adjusted R2, Predicted R2 and Adequate precision. R2 is known as the coefficient of determination, and indicates how close data are to the fitted regression line. It is a measure of the amount of reduction in the variability of response, predicted by the model, whereas adjusted and predicted R2 defines the predicting capability of model. All the three R2 values should be high and in a close range to ensure better predictability and adequacy of the model. The values of adequate precision, which is the measure of signal-to-noise ratio, for all responses in both sets are highly greater than 4, which

indicate that the model can be used to navigate the design space or to optimize the responses efficiently.

Table2: Abstracted ANOVA table for all responses

Material	Response	Significant terms	SS Model	DF	Lack of Fit	R^2	Adj-R^2	Pre-R^2	Adequate Precision
Aluminium	MRR	A,B,C,AB,AC ,BC,A^2,B^2,C^2	0.0094	9	Not sig	0.9967	0.9924	0.9771	50.68
	Hole Dia	A, B, C, AC , BC, A^2, C^2	0.1780	7	Not sig	0.9793	0.9632	0.8925	25.70
	Overcut	A, B, C, AC , BC, A^2, C^2	0.0622	7	Not sig	0.9810	0.9663	0.9240	25.75
Inconel	MRR	A,B,C,AB,AC ,BC,A^2,B^2,C^2	0.0033	9	Not sig	0.9938	0.9858	0.9443	36.98
	Hole Dia	A,B,C,AB,AC ,BC,A^2,B^2,C^2	0.1536	9	Not sig	0.9993	0.9984	0.9901	55.25
	Overcut	A, B, C, AC, A^2, C^2	0.0619	6	Not sig	0.9716	0.9546	0.9051	23.17

Design Expert software has been used to analyze the measured responses. Model significance test, significance test for each of the model terms and lack of fit test were carried out. A step wise regression method was selected to find out the significant model terms automatically and the resultant ANOVA tables for reduced quadratic model summarizing the analysis of variance for each response.

4.2.1 Analysis of variance for drilling in Aluminum Sheet

Analysis of variance of all the three output quality parameters has been studied for Aluminium sheet, which shows that for MRR the effects of Pulse frequency (A) and Duty cycle (B), Ultrasonic vibration frequency (C), interactions (AB), (BC) and (AC), and the quadratic effects of A^2, B^2 and C^2 are the significant model terms. Whereas for Hole diameter the effects of all the three process parameters, interaction (AC) and (BC) the quadratic effects of (A^2) and (C^2) are the significant model terms. The analysis of Overcut indicates that all the three main effects and Interaction effects of (AB) and (AC) and the quadratic effects of (A^2) and (C^2) are significant model terms. The abstracted ANOVA table for all the three responses in Aluminium sheet are presented in Table. Individual reduced ANOVA tables for each output variable are given in Appendix . The final regression models in terms of actual factors are given by

MRR = 0.715293 + 0.000191*A + 0.001639*B – 0.033366*C – 0.000465*AB – 0.00090*AC + 0.000461*BC + 0.00053*A^2 + 0.00021*B^2 + 0.000469*C^2

Hole Diameter = 6.05609 – 0.008005*A – 0.006152*B – 0.262558*C – 0.000312*AB + 0.000408*BC + 0.000326*A^2 + 0.003664*C^2

Overcut = 2.52525 – 0.000579*A + 0.0004246*B – 0.11228*C – 0.000019*AB – 0.000218*AC + 0.000151*A^2 + 0.001734*C^2

4.2.2 Analysis of variance for Drilling in Inconel Sheet

Analysis of variance of all the three output quality parameters has been studied for Inconel sheet, which shows that for MRR the effects of Pulse frequency (A) and Duty cycle (B), Ultrasonic vibration frequency (C), interactions (AB), (BC) and (AC), and the quadratic effects of (A^2), (B^2) and (C^2) are the significant model terms. Whereas for Hole diameter the effects of all the three process parameters, interaction (AB), (BC) and (AC) the quadratic effects of (A^2), (B^2) and (C^2) are the significant model terms. The analysis of Overcut indicates that all the three main effects and Interaction effect of (AC) and the quadratic effects of (A^2) and (C^2) are significant model terms. The abstracted ANOVA table for all the three responses in Inconel sheet are presented in Table. Individual reduced ANOVA tables for each output variable are given in Appendix B. The final regression models in terms of actual factors are given by

MRR = 0.513014 + 0.000132*A + 0.00054*B – 0.023115*C – 3.95597E-06*AB – 0.00058*AC + 0.000036*BC + 0.000034*A^2 – 5.12500E-0.6*B^2 + 0.000328*C^2

Hole Diameter = 4.58569 – 0.006818*A – 0.002699*B – 0.208778*C – 0.000035*AB – 0.000084*AC + 0.000233*BC + 0.000202*A^2 – 0.000026*B^2+ 0.002981*C^2

Overcut = 2.43186 – 0.001914*A + 0.003963*B – 0.118089*C – 0.000218*AC + 0.000155*A^2 + 0.001827*C^2

4.3 Experimental results

Voltage = 20V, IEG = 0.2 mm, Electrolyte concentration = 30 gm/lit, Pulse frequency = 5 khz, Duty cycle = 60, Ultrasonic vibration Frequency = 31 kHz, Top hole diameter = 1.744 mm, Bottom hole diameter = 0.972 mm, Overcut = 0.929 mm, MRR= 0.252 mg/min.

Groove images	
(a) 	(b) 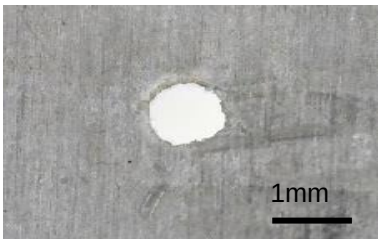

Fig17: (a) top view and (b) bottom view in drilled samples

4.4 Perturbation and Interaction plots: The perturbation plot helps to compare the effects of all the factors at a particular point in the design space. The response is plotted by changing only one factor over its range while holding all the other factors constant.

An interaction effect is the simultaneous effect of two or more independent variables on at least one dependent variable in which their joint effect is significantly greater (or significantly less) than the sum of the parts. An interaction plot displays the levels of one variable on the X axis and has a separate line for the means of each level of the other variable. The Y axis is the dependent variable.

The perturbation plot helps to compare the effects of all the factors at a particular point in the design space. The response is plotted by changing only one factor over its range while holding all the other factors constant. By default, Design-Expert sets the reference point at the midpoint (coded 0) of all the factors. You can change this to be any point by using the Factors Tool.

A steep slope or curvature in a factor shows that the response is sensitive to that factor. A relatively flat line shows insensitivity to change in that particular factor. If there are more than two factors, the perturbation plot could be used to find those factors that most affect the response. These influential factors are good choices for the axes on the contour plots.

The perturbation plots for MRR for Aluminum and Inconel sheets are shown below.

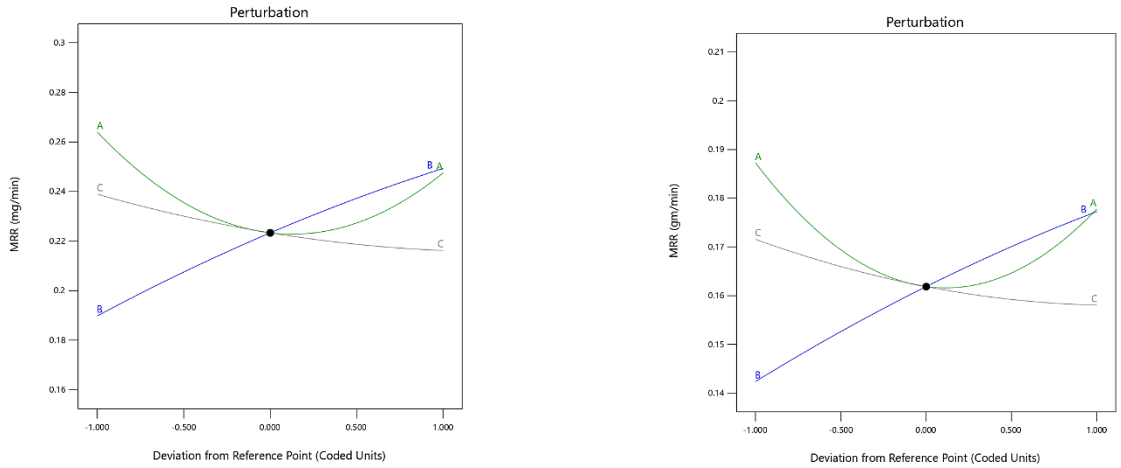

a. Aluminium sheet b. Inconel sheet

Fig.18: Perturbation plots

For both Aluminum and Inconel sheets, the MRR follows the same trend with all the three factors. MRR first increases with increase in pulse frequency but then after a certain point MRR decreases with the increase in pulse frequency. MRR increases as the Duty cycle increases.

The perturbation plots for Hole diameter for Aluminum and Inconel sheets are given below.

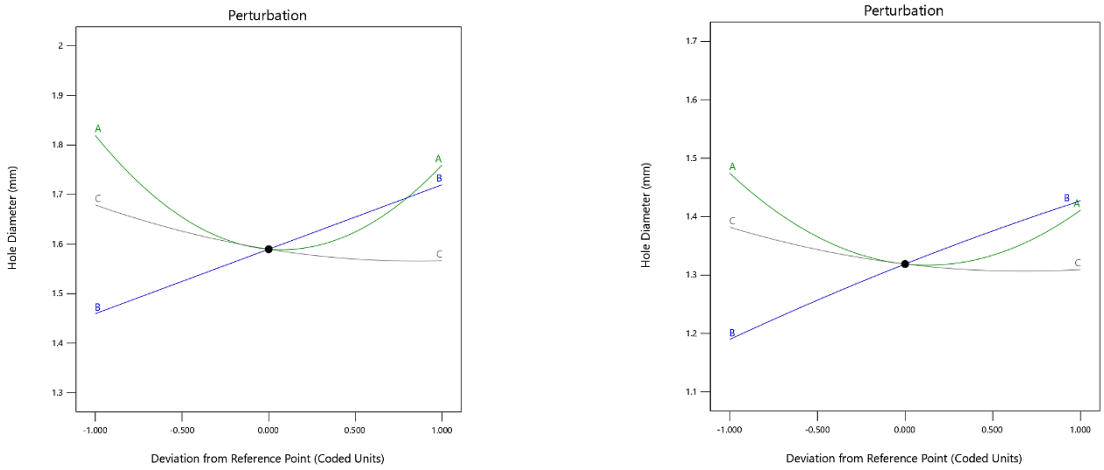

a. Aluminum sheet b. Inconel sheet

Fig.19: Perturbation plots

Hole diameters also follow the same trend as MRR but in case of Inconel sheet Hole diameter does not change much with change in pulse frequency as compared to the change in Hole diameter in Aluminum sheet.

The interaction Plots for overcut for Aluminium and Inconel sheets are shown below

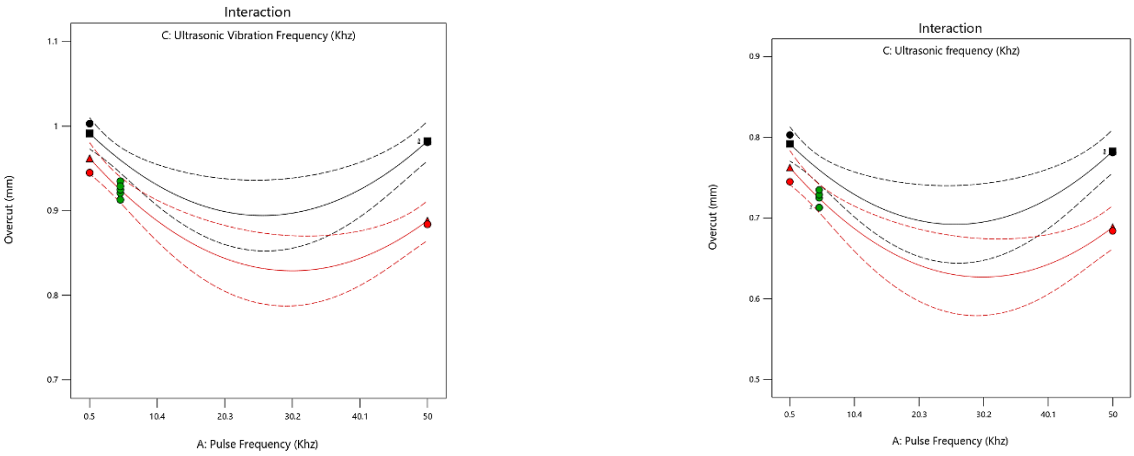

a. Aluminum sheet b. Inconel sheet

Fig.20: Interaction effects

The above figures show the interaction effect of Pulse frequency and Ultrasonic vibration frequency on the overcut.

With the increase in pulse frequency the overcut first slightly decreases then it slightly increases for aluminum an Inconel sheets

The perturbation plots for overcut for Aluminum and Inconel sheets are given below

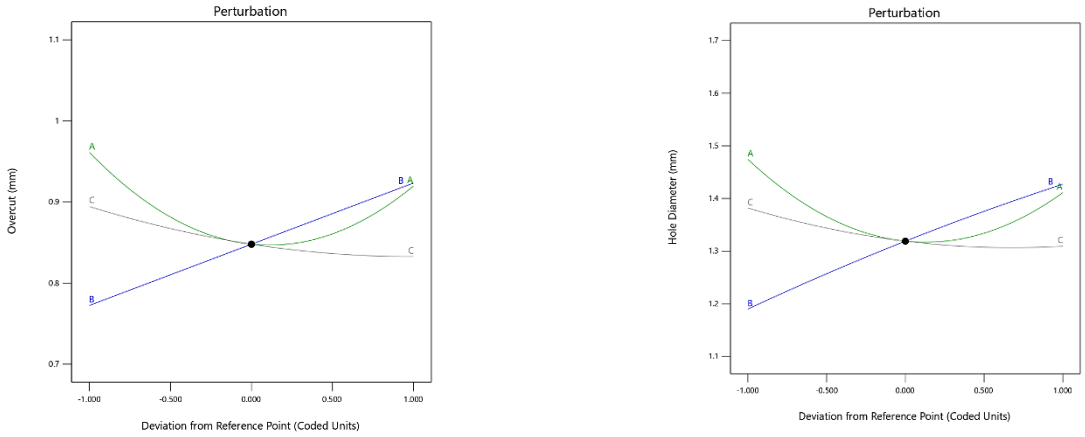

a Aluminum sheet b. Inconel sheet

Fig.21: Perturbation plots

All the three factors behave similarly for both the materials, and we can also observe that overcut decreases slightly with the increase in Ultrasonic vibration.

When the workpiece is subjected to vibration, IEG between electrodes changes periodically, so MRR increases, and also vibration improves flushing rate by removing trapped particles present in the slot. Vibration increases MRR so both top & bottom width values achieved here were more significant than previous pulse DC without vibration case.

The optimising is done using the Design of expert software by using the optimization option and by minimizing the overcut while maximizing the MRR gives us the optimum parameters for the machining.

Table 3: Optimum process parameters for maximizing MRR and Minimizing Overcut for Aluminum and Inconel sheet.

Material	Pulse Frequency	Duty Cycle	Ultrasonic frequency	MRR	Hole Diameter	Overcut
Aluminum	15	75	31.4	0.2342	1.7379	0.9337
Inconel	25	65	31.1	0.1972	1.419	0.7311

The validation was one by getting confirmation points, the optimised parameters another random value of input factors were used to perform the experiment and the experimental results were compare to the Design of experiments results and the error is within the margin

Table 4: Validation runs for drilling on both aluminium and Inconel sheet

Material	Pulse Frequency	Duty Cycle	Ultrasonic frequency	MRR	Hole Diameter	Overcut
Aluminum	15	75	31.4	0.2324	1.7422	0.9341
	10	70	30	0.2261	1.7216	0.9156
Inconel	25	65	31.1	0.1945	1.4921	0.7511
	10	70	30	0.1997	1.5016	0.7529

Contour plots: A contour plot provides a two-dimensional view in which all points that have the same response are connected to produce contour lines of constant responses. Contour plots are useful for investigating desirable response values and operating conditions.

A contour plot is the geometric illustration of a 3-D relationship in two dimensions, with X1 and X2 (independent variables) plotted on x- and y-scales and response values represented by contours (z-scale). Contour plots are useful for establishing the response values and operating conditions as required.

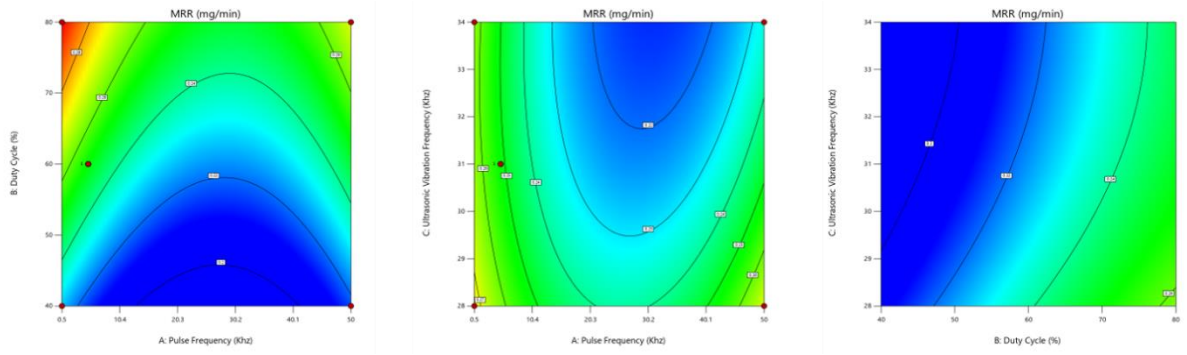

Fig.22 Contour plots of MRR for drilling in Aluminum sheet.

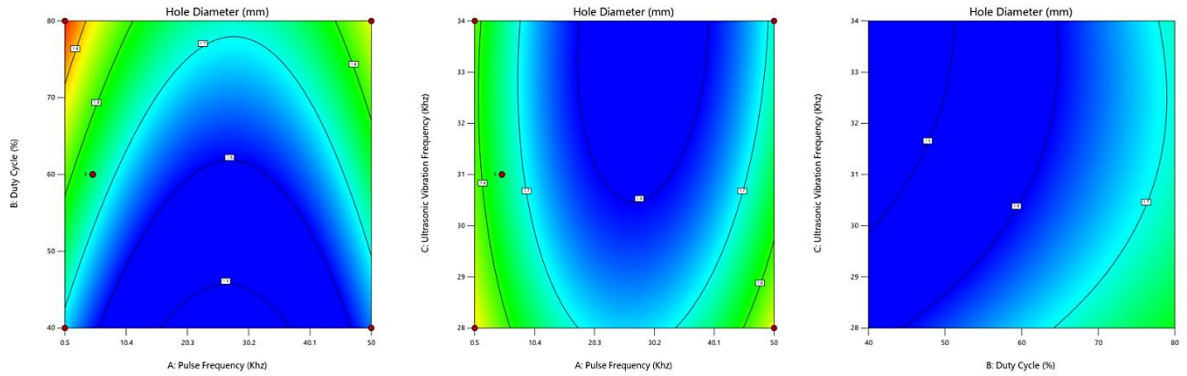

Fig.23 Contour plots of Hole diameter for drilling in Aluminum sheet.

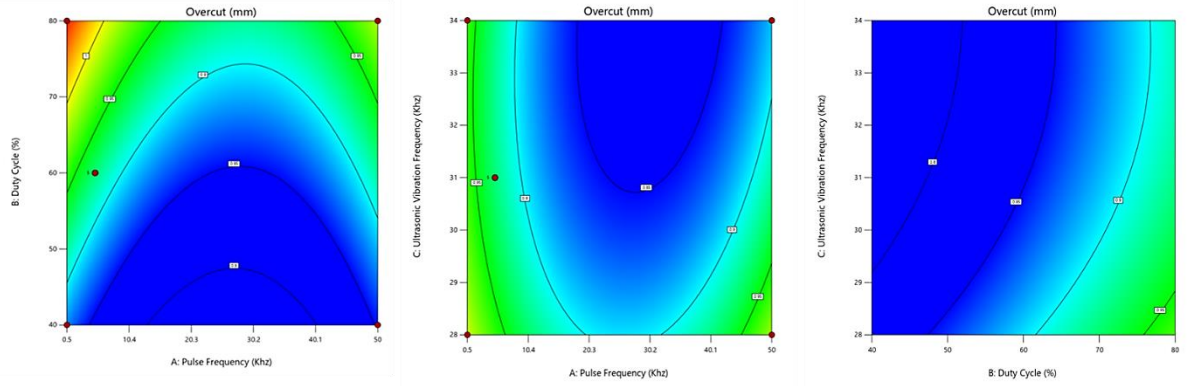

Fig.24 Contour plots of Overcut for drilling in Aluminum sheet.

The first graph showing MRR contour plot with pulse frequency and Duty cycle on X and Y axis is taken at the middle factor value of Ultrasonic frequency for drilling in Aluminum sheet. This gives us how MRR, Hole diameter and Overcut varies with the factor A and factor B at a constant factor C (middle value). All other graphs of Hole diameter and Overcut depict the same things graphically.

Here we can observe that the highest MRR is when Pulse frequency is low and the Duty cycle is high, and MRR decreases when Ultrasonic vibration frequency increases.

Overcut also follows a similar trend, as the MRR increases the overcut also increases.

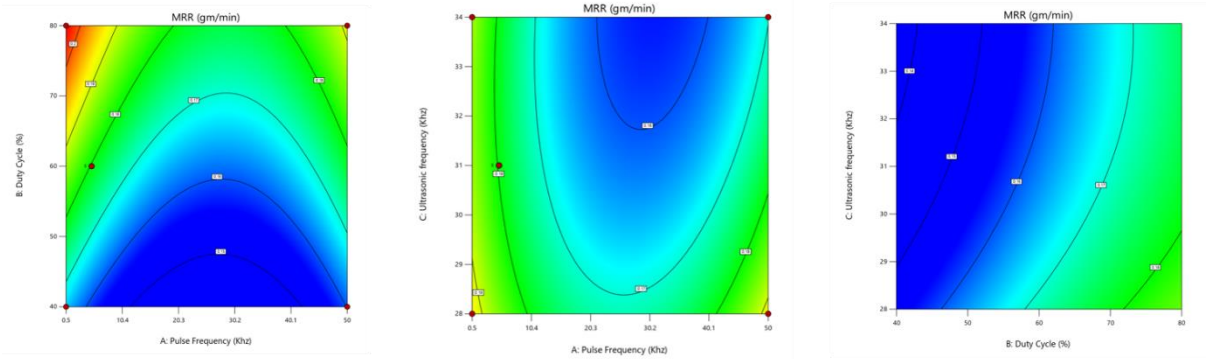

Fig.25 Contour plots of MRR for drilling in Inconel sheet.

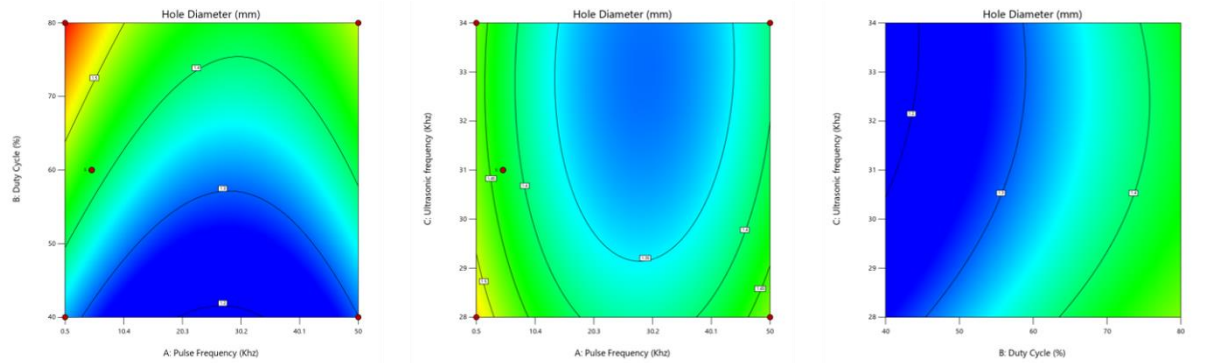

Fig.26 Contour plots of Hole diameter for drilling in Inconel sheet.

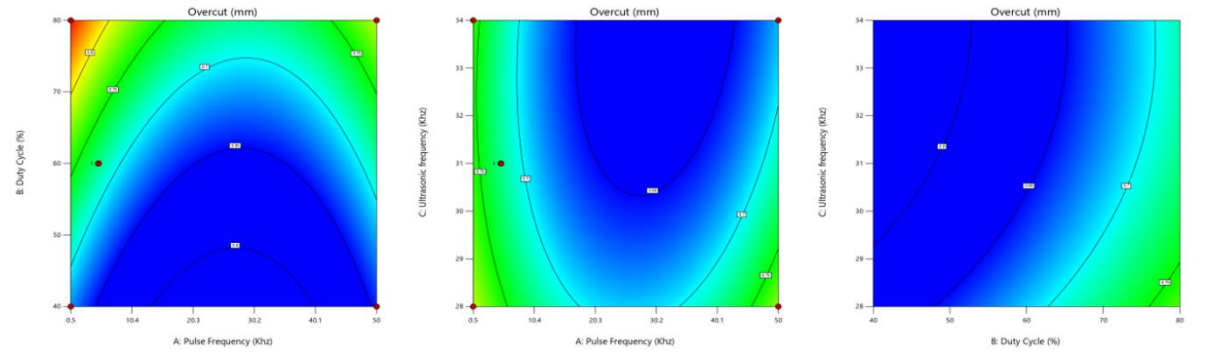

Fig.27 Contour plots of Overcut for drilling in Inconel sheet.

The first graph showing MRR contour plot with pulse frequency and Duty cycle on X and Y axis is taken at the middle factor value of Ultrasonic frequency for drilling in Inconel sheet. Here, we can observe that the highest MRR is when Pulse frequency is low and the Duty cycle is high, and MRR decreases when Ultrasonic vibration frequency increases. But we can also observe that MRR is considerably low in the case of Inconel.

Overcut also follows a similar trend, as the MRR increases the overcut also increases and as predictable the value of overcut is lower for holes drilled in Inconel sheet.

CHAPTER 5:
CONCLUSION AND FUTURE SCOPE

5.1 Conclusion

The current study investigates the drilling performance on aluminium and Inconel sheet through electro-jet machining under the application of pulsed DC and ultrasonic vibration. Further the drilling process was optimized through response surface methodology to obtain the set of parameters for minimum hole size and overcut along with maximum MRR.

- Higher pulse frequency and lower duty cycle results in the least amount of overcut and the lowest hole diameter, and as the Ultrasonic vibration frequency increases the hole diameter and the overcut decreases.
- Higher duty cycle and a lower pulse frequency gives higher MRR and as the Ultrasonic vibration frequency increases the MRR increases, this may be due to better flushing and periodic IEG change in Ultrasonic vibrations case.
- Holes drilled in Inconel sheets were found to have the lower amount of overcut and MRR as compared with holes drilled in Aluminum sheets.
- Response Surface methodology has shown that Duty cycle has the significant role in the operation as a the duty cycle increases, the MRR and overcut keeps on increasing.
- The optimum process parameters and response for Aluminum and Inconel are:

Material	Pulse Frequency	Duty Cycle	Ultrasonic frequency	MRR	Hole Diameter	Overcut
Aluminum	15	75	31.4	0.2342	1.7379	0.9337
Inconel	25	65	31.1	0.1972	1.419	0.7311

5.2 Future work

- Study the effect of the other process parameters like voltage, IEG, electrolyte concentration, feed rate on machining performances.
- Modify the MRR equation for Ultrasonic vibration case or finding out the amplitude of vibration will give us theoretical value of MRR in case of constant feed to the tool.
- Modifying the experimental setup so that we can give feed rates as small as 0.1mm/min to the tool while giving Ultrasonic vibrations to the workpiece.
- Performing the same experiment of thicker sheets and observing the range of MRR, hole diameter and the overcut.

CHAPTER 6:
REFERENCES

1) Zhang, C., Yao, J., Zhang, C., Chen, X., Liu, J., & Zhang, Y. (2020). Electrochemical milling of narrow grooves with high aspect ratio using a tube electrode. *Journal of Materials Processing Technology*, *282*, 116695.
2) Heiwdy et al. Modelling the performance of ECM assisted by low frequency vibrations, Journal of Materials Processing Technology 189 (2007) 466–472.
3) Zhu, X., Liu, Y., Zhang, J., Wang, K., & Kong, H. (2020). Ultrasonic-assisted electrochemical drill-grinding of small holes with high-quality. *Journal of advanced research*, *23*, 151-161.
4) Wang, M., Zhang, Y., He, Z., & Peng, W. (2016). Deep micro-hole fabrication in EMM on stainless steel using disk micro-tool assisted by ultrasonic vibration. *Journal of Materials Processing Technology*, *229*, 475-483.
5) Ebeid, S. J., Hewidy, M. S., El-Taweel, T. A., & Youssef, A. H. (2004). Towards higher accuracy for ECM hybridized with low-frequency vibrations using the response surface methodology. *Journal of Materials Processing Technology*, *149*(1-3), 432-438.
6) Bilgi, D. S., Kumar, R., Jain, V. K., & Shekhar, R. (2008). Predicting radial overcut in deep holes drilled by shaped tube electrochemical machining. *The International Journal of Advanced Manufacturing Technology*, *39*(1), 47-54.
7) Kumar, P., Jadhav, P., Beldar, M., Jadhav, D. B., & Sawant, A. (2018). Review paper on ECM, PECM and ultrasonic assisted PECM. *Materials Today: Proceedings*, *5*(2), 6381-6390.

8) Patil, K. D., Jadhav, D. B., & Kharche, W. G. Experimental study of MRR of ECM on stainless steel 200 material. *International Journal of Engineering Research and General Science*.
9) Tarakesh Dalabehera (2020) Development and experimental analysis towards Electro-jet micro-milling of advanced metals (thin sheets)
10) Bilgi, D. S., Kumar, R., Jain, V. K., & Shekhar, R. (2008). Predicting radial overcut in deep holes drilled by shaped tube electrochemical machining. The International Journal of Advanced Manufacturing Technology, 39(1), 47-54.
11) Kumar, P., Jadhav, P., Beldar, M., Jadhav, D. B., & Sawant, A. (2018). Review paper on ECM, PECM and ultrasonic assisted PECM. Materials Today: Proceedings, 5(2), 6381-6390.
12) Patil, K. D., Jadhav, D. B., & Kharche, W. G. Experimental study of MRR of ECM on stainless steel 200 material. International Journal of Engineering Research and General Science.
13) Mittal, D., Garg, M. P., & Khanna, R. (2011). An investigation of the effect of process parameters on MRR in turning of pure titanium(grade-2). International Journal of Engineering Science and Technology, 3(8).
14) da Silva Neto, J. C., Da Silva, E. M., & Da Silva, M. B. (2006). Intervening variables in electrochemical machining. Journal of Materials Processing Technology, 179(1-3), 92-96.
15) Bhattacharyya, B., & Sorkhel, S. K. (1999). Investigation for controlled electrochemical machining through response surface methodology-based approach. Journal of Materials Processing Technology, 86(1-3), 200-207.
16) Chakradhar, D., & Gopal, A. V. (2011). Multi-objective optimization of electrochemical machining of EN31 steel by grey relational analysis. International Journal of Modelling and optimization, 1(2), 113.

Appendix

ANOVA for Quadratic model for Drilling in Aluminum sheet

Response 1: MRR

Source	Sum of Squares	df	Mean Square	F-value	p-value	
Model	0.0094	9	0.0010	233.98	< 0.0001	significant
A-Pulse Frequency	0.0005	1	0.0005	121.79	< 0.0001	
B-Duty Cycle	0.0057	1	0.0057	1267.92	< 0.0001	
C-Ultrasonic Vibration Frequency	0.0008	1	0.0008	184.82	< 0.0001	
AB	0.0001	1	0.0001	13.10	0.0085	
AC	0.0002	1	0.0002	53.61	0.0002	
BC	0.0000	1	0.0000	6.77	0.0354	
A^2	0.0004	1	0.0004	80.11	< 0.0001	
B^2	0.0001	1	0.0001	13.42	0.0080	
C^2	0.0001	1	0.0001	16.81	0.0046	
Residual	0.0000	7	4.471E-06			
Lack of Fit	6.495E-06	3	2.165E-06	0.3492	0.7930	not significant
Pure Error	0.0000	4	6.200E-06			
Cor Total	0.0094	16				

P-values less than 0.0500 indicate model terms are significant. In this case A, B, C, AB, AC, BC, A^2, B^2, C^2 are significant model terms. Values greater than 0.1000 indicate the model terms are not significant. If there are many insignificant model terms (not counting those required to support hierarchy), model reduction may improve your model.

The **Lack of Fit F-value** of 0.35 implies the Lack of Fit is not significant relative to the pure error. There is a 79.30% chance that a Lack of Fit F-value this large could occur due to noise. Non-significant lack of fit is good -- we want the model to fit.

ANOVA for Reduced Quadratic model for drilling in Aluminium Sheet

Response 2: Hole Diameter

Source	Sum of Squares	df	Mean Square	F-value	p-value	
Model	0.1780	7	0.0254	60.80	< 0.0001	significant
A-Pulse Frequency	0.0071	1	0.0071	16.93	0.0026	
B-Duty Cycle	0.1355	1	0.1355	323.85	< 0.0001	
C-Ultrasonic Vibration Frequency	0.0203	1	0.0203	48.56	< 0.0001	
AC	0.0029	1	0.0029	6.85	0.0279	
BC	0.0024	1	0.0024	5.74	0.0402	
A^2	0.0136	1	0.0136	32.55	0.0003	
C^2	0.0046	1	0.0046	10.98	0.0090	
Residual	0.0038	9	0.0004			
Lack of Fit	0.0032	5	0.0006	4.57	0.0831	not significant
Pure Error	0.0006	4	0.0001			
Cor Total	0.1818	16				

Factor coding is **Coded**.
Sum of squares is **Type III - Partial**
The **Model F-value** of 60.80 implies the model is significant. There is only a 0.01% chance that an F-value this large could occur due to noise.
P-values less than 0.0500 indicate model terms are significant. In this case A, B, C, AC, BC, A^2, C^2 are significant model terms. Values greater than 0.1000 indicate the model terms are not significant. If there are many insignificant model terms (not counting those required to support hierarchy), model reduction may improve your model.
The **Lack of Fit F-value** of 4.57 implies there is a 8.31% chance that a Lack of Fit F-value this large could occur due to noise. Lack of fit is bad -- we want the model to fit. This relatively low probability (<10%) is troubling.

ANOVA for Reduced Quadratic model for drilling in Aluminum sheet

Response 3: Overcut

Source	Sum of Squares	df	Mean Square	F-value	p-value	
Model	0.0622	7	0.0089	66.52	< 0.0001	significant
A-Pulse Frequency	0.0034	1	0.0034	25.80	0.0007	
B-Duty Cycle	0.0364	1	0.0364	272.75	< 0.0001	
C-Ultrasonic Vibration Frequency	0.0061	1	0.0061	45.67	< 0.0001	
AB	0.0005	1	0.0005	3.44	0.0965	
AC	0.0014	1	0.0014	10.49	0.0102	
A^2	0.0029	1	0.0029	21.86	0.0012	
C^2	0.0010	1	0.0010	7.70	0.0216	
Residual	0.0012	9	0.0001			
Lack of Fit	0.0009	5	0.0002	2.69	0.1793	not significant
Pure Error	0.0003	4	0.0001			
Cor Total	0.0634	16				

Factor coding is **Coded**.
Sum of squares is **Type III - Partial**
The **Model F-value** of 66.52 implies the model is significant. There is only a 0.01% chance that an F-value this large could occur due to noise.
P-values less than 0.0500 indicate model terms are significant. In this case A, B, C, AC, A^2, C^2 are significant model terms. Values greater than 0.1000 indicate the model terms are not significant. If there are many insignificant model terms (not counting those required to support hierarchy), model reduction may improve your model.
The **Lack of Fit F-value** of 2.69 implies the Lack of Fit is not significant relative to the pure error. There is a 17.93% chance that a Lack of Fit F-value this large could occur due to noise.
Non-significant lack of fit is good -- we want the model to fit.

ANOVA for Quadratic model for drilling in Inconel Sheet

Response 1: MRR

Source	Sum of Squares	df	Mean Square	F-value	p-value	
Model	0.0033	9	0.0004	124.51	< 0.0001	significant
A-Pulse Frequency	0.0002	1	0.0002	61.86	0.0001	
B-Duty Cycle	0.0019	1	0.0019	667.41	< 0.0001	
C-Ultrasonic frequency	0.0003	1	0.0003	100.04	< 0.0001	
AB	0.0000	1	0.0000	7.02	0.0330	
AC	0.0001	1	0.0001	33.69	0.0007	
BC	0.0000	1	0.0000	5.48	0.0517	
A^2	0.0001	1	0.0001	49.87	0.0002	
B^2	0.0000	1	0.0000	6.06	0.0433	
C^2	0.0000	1	0.0000	12.56	0.0094	
Residual	0.0000	7	2.918E-06			
Lack of Fit	5.224E-06	3	1.741E-06	0.4583	0.7262	not significant
Pure Error	0.0000	4	3.800E-06			
Cor Total	0.0033	16				

Factor coding is **Coded**.

Sum of squares is **Type III - Partial**

The **Model F-value** of 124.51 implies the model is significant. There is only a 0.01% chance that an F-value this large could occur due to noise.

P-values less than 0.0500 indicate model terms are significant. In this case A, B, C, AB, AC, A^2, B^2, C^2 are significant model terms. Values greater than 0.1000 indicate the model terms are not significant. If there are many insignificant model terms (not counting those required to support hierarchy), model reduction may improve your model.

The **Lack of Fit F-value** of 0.46 implies the Lack of Fit is not significant relative to the pure error. There is a 72.62% chance that a Lack of Fit F-value this large could occur due to noise. Non-significant lack of fit is good -- we want the model to fit.

ANOVA for Quadratic model for drilling in Inconel sheet

Response 2: Hole Diameter

Source	Sum of Squares	df	Mean Square	F-value	p-value	
Model	0.1504	9	0.0167	1085.07	< 0.0001	significant
A-Pulse Frequency	0.0080	1	0.0080	519.59	< 0.0001	
B-Duty Cycle	0.0900	1	0.0900	5843.74	< 0.0001	
C-Ultrasonic frequency	0.0084	1	0.0084	547.09	< 0.0001	
AB	0.0016	1	0.0016	101.84	< 0.0001	
AC	0.0002	1	0.0002	13.39	0.0081	
BC	0.0008	1	0.0008	50.91	0.0002	
A^2	0.0052	1	0.0052	339.06	< 0.0001	
B^2	0.0005	1	0.0005	29.72	0.0010	
C^2	0.0030	1	0.0030	196.75	< 0.0001	
Residual	0.0001	7	0.0000			
Lack of Fit	0.0001	3	0.0000	6.15	0.0558	not significant
Pure Error	0.0000	4	4.800E-06			
Cor Total	0.1505	16				

Factor coding is **Coded**.
Sum of squares is **Type III - Partial**
The **Model F-value** of 1085.07 implies the model is significant. There is only a 0.01% chance that an F-value this large could occur due to noise.
P-values less than 0.0500 indicate model terms are significant. In this case A, B, C, AB, AC, BC, A^2, B^2, C^2 are significant model terms. Values greater than 0.1000 indicate the model terms are not significant. If there are many insignificant model terms (not counting those required to support hierarchy), model reduction may improve your model.
The **Lack of Fit F-value** of 6.15 implies there is a 5.58% chance that a Lack of Fit F-value this large could occur due to noise. Lack of fit is bad -- we want the model to fit. This relatively low probability (<10%) is troubling.

ANOVA for Reduced Quadratic model for drilling in Inconel sheet

Response 3: Overcut

Source	Sum of Squares	df	Mean Square	F-value	p-value	
Model	0.0619	6	0.0103	57.07	< 0.0001	significant
A-Pulse Frequency	0.0034	1	0.0034	19.04	0.0014	
B-Duty Cycle	0.0502	1	0.0502	277.79	< 0.0001	
C-Ultrasonic frequency	0.0061	1	0.0061	33.71	0.0002	
AC	0.0014	1	0.0014	7.74	0.0194	
A^2	0.0031	1	0.0031	17.03	0.0021	
C^2	0.0011	1	0.0011	6.31	0.0308	
Residual	0.0018	10	0.0002			
Lack of Fit	0.0014	6	0.0002	2.47	0.2000	not significant
Pure Error	0.0004	4	0.0001			
Cor Total	0.0637	16				

Factor coding is **Coded**.

Sum of squares is **Type III - Partial**

The **Model F-value** of 57.07 implies the model is significant. There is only a 0.01% chance that an F-value this large could occur due to noise.

P-values less than 0.0500 indicate model terms are significant. In this case A, B, C, AC, A^2, C^2 are significant model terms. Values greater than 0.1000 indicate the model terms are not significant. If there are many insignificant model terms (not counting those required to support hierarchy), model reduction may improve your model.

The **Lack of Fit F-value** of 2.47 implies the Lack of Fit is not significant relative to the pure error. There is a 20.00% chance that a Lack of Fit F-value this large could occur due to noise.

Non-significant lack of fit is good -- we want the model to fit.